

Influence of molybdenum doping on the switching characteristic in silicon oxide-based resistive switching memory

Yu-Ting Chen, Ting-Chang Chang, Jheng-Jie Huang, Hsueh-Chih Tseng, Po-Chun Yang, Ann-Kuo Chu, Jyun-Bao Yang, Hui-Chun Huang, Der-Shin Gan, Ming-Jinn Tsai, and Simon M. Sze

Citation: *Applied Physics Letters* **102**, 043508 (2013); doi: 10.1063/1.4790277

View online: <http://dx.doi.org/10.1063/1.4790277>

View Table of Contents: <http://scitation.aip.org/content/aip/journal/apl/102/4?ver=pdfcov>

Published by the [AIP Publishing](#)

Articles you may be interested in

[Forming-free resistive switching characteristics of 15nm-thick multicomponent oxide](#)

Appl. Phys. Lett. **103**, 252904 (2013); 10.1063/1.4852059

[Conductance quantization in oxygen-anion-migration-based resistive switching memory devices](#)

Appl. Phys. Lett. **103**, 043510 (2013); 10.1063/1.4816747

[Performance and characteristics of double layer porous silicon oxide resistance random access memory](#)

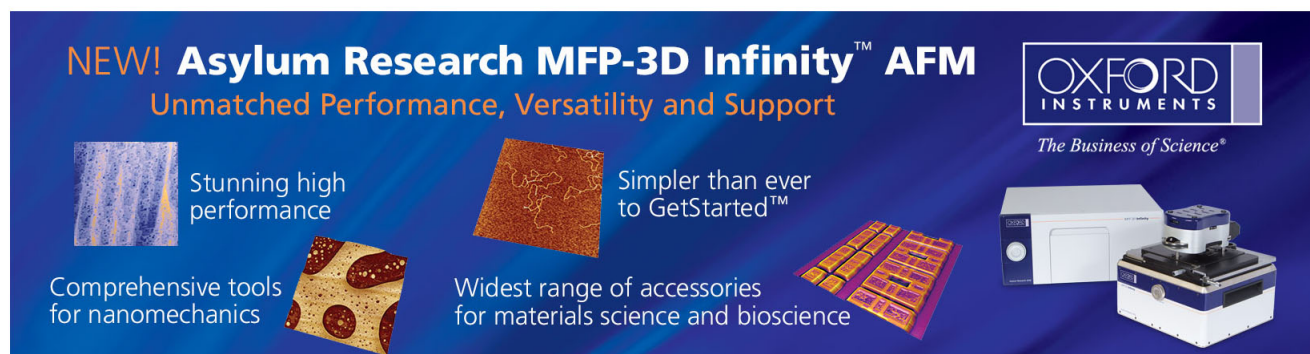
Appl. Phys. Lett. **102**, 253509 (2013); 10.1063/1.4812474

[Understanding the resistive switching characteristics and mechanism in active SiO_x-based resistive switching memory](#)

J. Appl. Phys. **112**, 123702 (2012); 10.1063/1.4769218

[Study of polarity effect in SiO_x-based resistive switching memory](#)

Appl. Phys. Lett. **101**, 052111 (2012); 10.1063/1.4742894

The advertisement features a dark blue background with white and orange text. At the top left, it reads 'NEW! Asylum Research MFP-3D Infinity™ AFM' in large white letters, followed by 'Unmatched Performance, Versatility and Support' in orange. On the right, the Oxford Instruments logo is shown with the tagline 'The Business of Science®'. Below the text are several images: a blue textured surface, a brown textured surface, a yellow and red patterned surface, and a photograph of the MFP-3D Infinity AFM instrument. Text boxes describe the instrument's capabilities: 'Stunning high performance', 'Simpler than ever to GetStarted™', 'Comprehensive tools for nanomechanics', and 'Widest range of accessories for materials science and bioscience'.

Influence of molybdenum doping on the switching characteristic in silicon oxide-based resistive switching memory

Yu-Ting Chen,¹ Ting-Chang Chang,^{1,2,a)} Jheng-Jie Huang,² Hsueh-Chih Tseng,² Po-Chun Yang,¹ Ann-Kuo Chu,¹ Jyun-Bao Yang,¹ Hui-Chun Huang,³ Der-Shin Gan,³ Ming-Jinn Tsai,⁴ and Simon M. Sze^{2,5}

¹Department of Photonics, National Sun Yat-Sen University, Kaohsiung 804, Taiwan

²Department of Physics and Center for Nanoscience and Nanotechnology, National Sun Yat-Sen University, Kaohsiung 804, Taiwan

³Department of Materials Science and Engineering, National Sun Yat-Sen University, Kaohsiung 804, Taiwan

⁴Electronics and Optoelectronics Research Laboratory, Industrial Technology Research Institute, Chutung, Hsinchu 310, Taiwan

⁵Department of Electronics Engineering, National Chiao Tung University, Hsinchu 300, Taiwan

(Received 8 October 2012; accepted 21 January 2013; published online 1 February 2013)

This report compares Mo-doped and undoped SiO₂ thin films of a similar thickness as well as MoO_x. The Mo-doped SiO₂ film exhibited switching behavior after the forming process, unlike the undoped SiO₂ film. Through material analyses, a self-assembled layer is observed in the Mo-doped SiO₂ film. Due to the formation of this layer, the thickness required to be broken down is effectively reduced. Subsequently, the occurrence of the switching behavior in the thinner SiO₂ film further confirmed the supposition. A comparison of the two switching behaviors shows that SiO₂ dominates the switching characteristic of the Mo-doped SiO₂. © 2013 American Institute of Physics. [<http://dx.doi.org/10.1063/1.4790277>]

Due to device size scaling requirements, conventional charge storage based memory structures, such as nanocrystal and SONOS, have encountered data storage problems.^{1–3} In recent years, resistive random access memory (ReRAM) has attracted considerable attention as a solution due to its superior advantages.^{4,5} Resistive switching (RS) characteristics have been discovered in various materials.^{6–10} Due to their well-developed production processes, well-known material characteristics and wide applications in Si-based thin film, SiO₂, or Si-based materials are considered to have the most potential as candidates for ReRAM. However, the RS behavior rarely occurs in SiO₂ unless metal doping or solid electrolyte electrodes are employed.^{11,12} In this paper, this resistive switching issue is investigated in a device utilizing molybdenum-doped SiO₂ film. In addition, molybdenum oxide may transform to molybdenum nanocrystals due to the thermal effect which has been induced by the forming process.^{13,14} This nanocrystal formation and consequent generation of additional oxygen ions per molybdenum atom have been shown to improve the RS performance.⁸

In this work, standard lithography and reactive ion etching were used to pattern the contact-holes of the cells on the TiN bottom electrode. A 20 nm-thick Mo-doped SiO₂ film (sample A) was deposited by sputtering a MoSi₂ target in O₂ ambient at room temperature. A 200 nm-thick Pt top electrode was subsequently stacked. Finally, the devices were completed after a lift-off process. The diagram of the structure is shown in Fig. 1(a). An additional 20 nm-thick MoO_x film as well as 23 nm- and 12 nm-thick SiO₂ (sample B) films were fabricated with the same structure.

The RS characteristics were measured by biasing from TiN and grounding at Pt by using an Agilent B1500 semi-

conductor parameter analyzer. During the forming process, the leakage current of the film increased dramatically and achieved low resistance state (LRS) due to the formation of the conductive filament (CF). When negative voltage was applied, the high resistance state (HRS) was obtained by a gradual increase of resistance during the reset process. Subsequently, LRS can be switched back through the set process by applying positive voltage. The morphology and the components of the films were analyzed by transmission electron microscope (TEM) and X-ray photoelectron spectroscopy (XPS), respectively.

After the forming process by applying positive bias, the RS phenomenon is activated, as shown in the left inset of Fig. 1(b). A stable and repeatable RS behavior is presented in sample A, as shown in Fig. 1(b). The switching mechanism is dominated by the oxygen vacancy generation/recombination as is demonstrated by the relationship between CF resistance and temperature for LRS, shown in the right inset of Fig. 1(a).^{15,16} Through the material analyses of the X-ray photoelectron spectrum, the components of the film can be further confirmed by the Lorentzian-Gaussian fitting. In the photoelectron spectrum of Si 2p_{3/2}, only one peak, that attributed to the SiO₂ (103 eV), is discovered, as shown in Fig. 1(c).¹⁷ In the photoelectron spectrum of O 1s, the spectrum can be separated into two peaks, located at 530.6 eV and 532.4 eV, shown in Fig. 1(d). According to previous research, these two peaks can be assigned as the bonds of MoO₃ and SiO₂.^{17,18}

In order to investigate the RS phenomenon in the Mo-doped SiO₂ film, the same structure with 20 nm-thick MoO_x and SiO₂ films was similarly analyzed. The RS characteristic of MoO_x is shown in Fig. 2(a). Obviously, the switching behavior is very unstable and fails to switch after several tens of cycles, as shown in the left inset of Fig. 2(a).

^{a)}tcchang@mail.phys.nsysu.edu.tw.

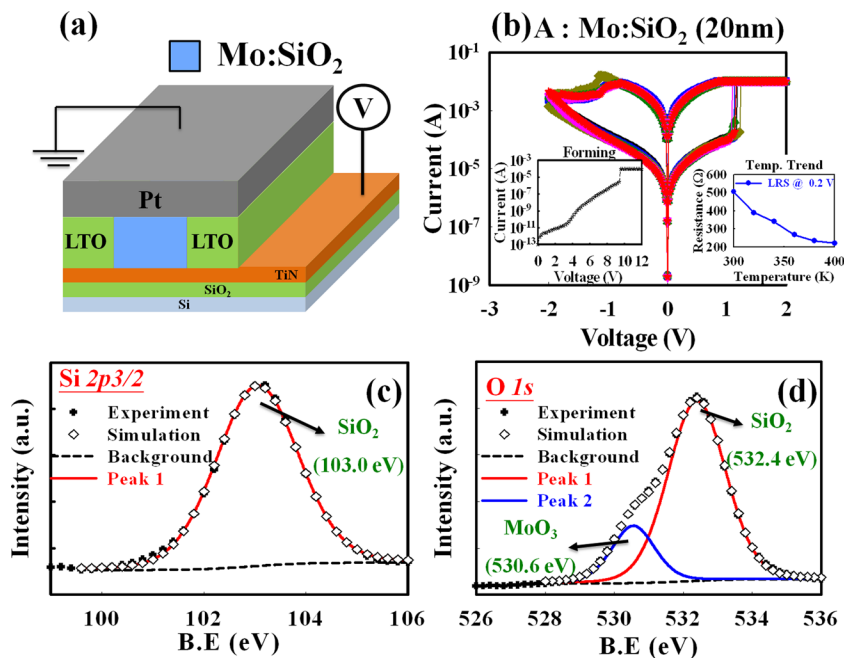


FIG. 1. (a) Structural diagram and (b) switching behavior of the device using Mo-doped SiO₂ film. XPS analyses of (c) Si 2p_{3/2}, and (d) O 1s. The left and right insets of (b) show the forming characteristic and the temperature-dependence trend of LRS, respectively.

In addition, the switching mechanism of MoO_x is due to the rupture and formation of the metallic filament, as indicated by the proportional relationship between the resistance and the temperature at LRS, shown in the right inset of Fig. 2(a).^{19–21} However, the structure with 20 nm-thick SiO₂ fails to be activated during the forming process. The breakdown behavior does not occur even though voltage is applied up to 20 V, as shown in Fig. 2(b). As a result, TEM analysis is employed to determine the difference in the forming process between the Mo-doped SiO₂ and pure SiO₂ films. The TEM image of sample A shown in Fig. 2(c) clearly shows a dark region, indicating that a self-assembled layer exists in the

film. The self-assembled layer can be confirmed as MoO₃ according to the result of XPS analyses. The thickness of the film required to undergo breakdown might then be reduced due to the existence of the nearly 5 nm-thick self-assembled MoO₃ layer.

In order to clarify this supposition, a 12-nm-thick SiO₂ film is used to cancel out the influence of the self-assembled MoO₃ layer (5 nm). After the reduction in the thickness of the SiO₂ film (sample B), a stable RS characteristic is obtained when the device undergoes the forming process, as shown in Fig. 3(a). The right inset of Fig. 3(a) shows the inversely proportional relationship between the resistance in

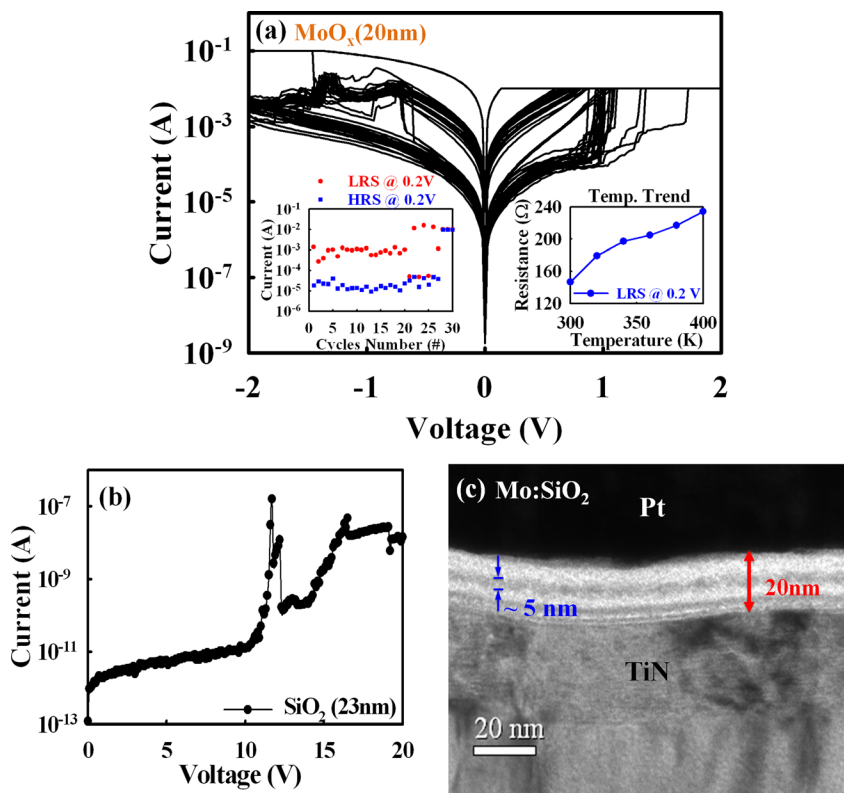


FIG. 2. (a) The unstable switching characteristic of 20 nm-thick MoO_x. (b) Activation failure during the forming process for 23 nm-thick SiO₂ film. (c) TEM image of Mo-doped SiO₂ film. The left and right insets of (a) show the switching stability and metallic temperature behavior of LRS, respectively.

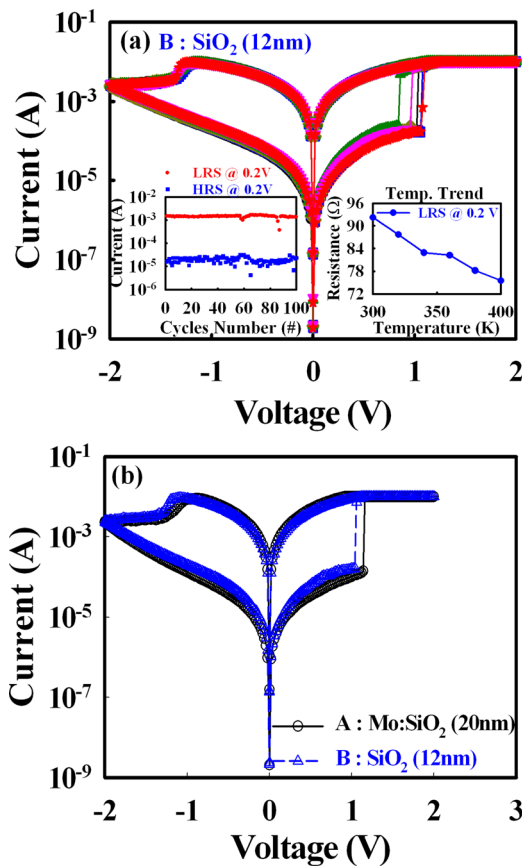


FIG. 3. (a) The repeatable switching characteristic of 12 nm-thick SiO₂ film and (b) comparison with the switching characteristic of 20 nm-thick Mo-doped SiO₂. Left inset of (a) shows stable switching behavior; right inset of (a) presents temperature behavior of LRS showing that oxygen vacancies dominate the conduction mechanism.

LRS and ambient temperature, which exhibits the same trend as in sample A. In addition, the RS characteristics of sample A and sample B are compared in Fig. 3(b), which shows that

the switching behavior of the device with Mo-doped SiO₂ film is nearly the same as that of SiO₂, including the switching voltage and ON/OFF ratio. Therefore, this indicates that switching characteristic of sample A is dominated by SiO₂.

However, in addition to affecting the forming process by reducing the thickness required for breakdown, the doped molybdenum also influences RS behavior. The current statistics in Fig. 4(a) for HRS and LRS extracted at 0.2 V for the two samples show that a lower HRS current occurs in sample A. Since the HRS current is an indicator of the degree of repair for the switching regime of the CF, called switching layer (SL),²² a lower HRS current shows that higher performance of the repaired SL is obtained, which might be caused by the existence of more oxygen ions to repair the SL during the reset process.^{23,24} Next, conduction mechanism analyses are employed and indicate that the conduction mechanism is Schottky emission from -0.48 V to -1 V in HRS for sample A, as shown by the linear fitting between current and root of voltage ($I-V^{1/2}$). However, Poole-Frenkel emission instead dominates the conduction mechanism along a similar range (-0.2 V to -0.9 V) for sample B, as shown in Fig. 4(b). It is notable that the conduction mechanisms of Fowler-Nordheim tunneling and trap assisted tunneling (TAT) are not supported by fitting analyses, only Poole-Frenkel emission (not shown). These results indicate that the distances of the trap states in the SL, which are attributed to the unrepaired oxygen vacancies, might be too far for charges to transport by tunneling. Therefore, charges transport by electric field assisted thermal emission. Furthermore, the conduction mechanism transfer from Poole-Frenkel (sample B) to Schottky emission (sample A) is caused by the improved SL repair during the reset process. MoO₃, as indicated by the XPS analysis, can provide three more oxygen ions by breaking all of the bonds of Mo-O during the forming process, with a schematic of the processes shown in

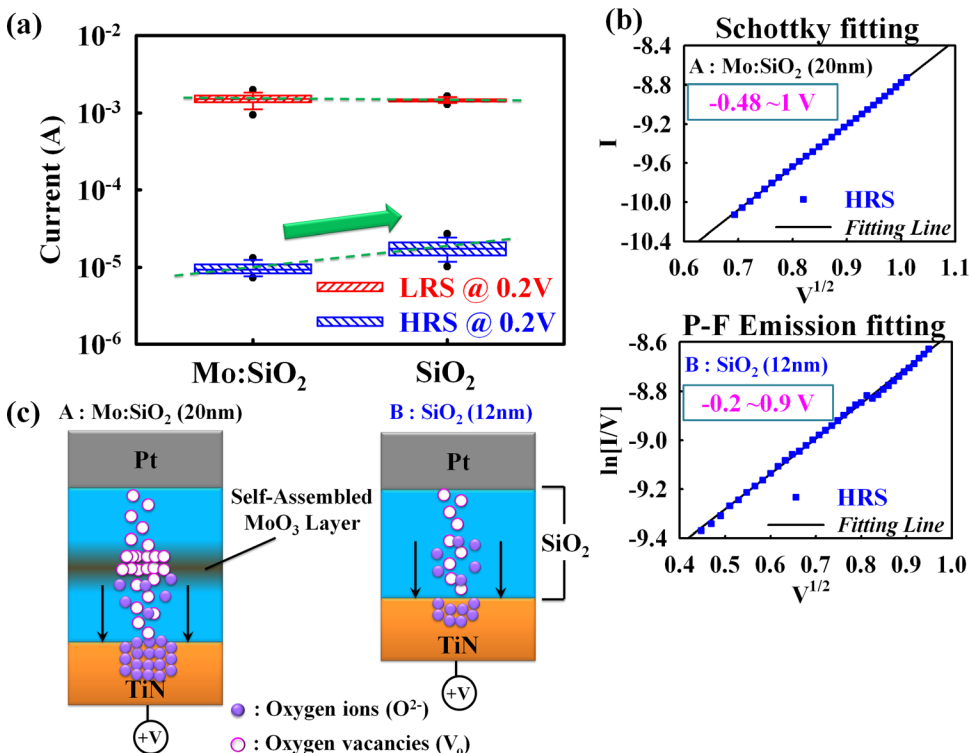


FIG. 4. (a) Statistics for the LRS and HRS in samples A and B. (b) Conduction mechanisms of samples A and B in HRS are, respectively, dominated by Schottky and Poole-Frenkel emissions. (c) Schematic diagrams to illustrate the behaviors after the forming process.

Fig. 4(c). As a result, the additional oxygen ions in sample A improve the repaired performance for the SL during the reset process. The higher quality interfacial SL leads to a lower HRS current and the conduction mechanism being dominated by Schottky emission.

In summary, although switching behavior can be obtained in the Mo-doped SiO₂ film, the RS characteristic is not dominated by the MoO_x. Because the 20 nm-thick SiO₂ film failed in the forming process, a TEM image of the Mo-doped SiO₂ film was examined and showed that the self-assembled molybdenum oxide layer reduces the thickness of the film required to be broken down. A thinner SiO₂ film exhibited a stable RS characteristic nearly the same as that of the Mo-doped SiO₂ film. Therefore, the switching behavior of the Mo-doped SiO₂ film is in fact dominated by SiO₂. The change in conduction mechanism in HRS between the two devices is due to the additional oxygen ions provided by MoO₃.

This work was performed at National Science Council Core Facilities Laboratory for Nano-Science and Nano-Technology in Kaohsiung-Pingtung area and was supported by the National Science Council of the Republic of China under Contract NSC 101-2120-M-110-002.

¹J. Lu, T. C. Chang, Y. T. Chen, J. J. Huang, P. C. Yang, S. C. Chen, H. C. Huang, D. S. Gan, N. J. Ho, Y. Shi, and A. K. Chu, *Appl. Phys. Lett.* **96**, 262107 (2010).

²T. C. Chang, F. Y. Jian, S. C. Chen, and Y. T. Tsai, *Mater. Today* **14**, 608 (2011).

³S. C. Chen, T. C. Chang, P. T. Liu, Y. C. Wu, P. S. Lin, B. H. Tseng, J. H. Shy, S. M. Sze, C. Y. Chang, and C. H. Lien, *IEEE Trans. Electron Device Lett.* **28**, 809 (2007).

⁴M. Fujimoto, H. Koyama, Y. Nishi, and T. Suzuki, *Appl. Phys. Lett.* **91**, 223504 (2007).

⁵H. Shima, F. Takano, H. Muramatsu, H. Akinaga, Y. Tamai, I. H. Inoue, and H. Takagi, *Appl. Phys. Lett.* **93**, 113504 (2008).

⁶D. Choi, D. Lee, H. Sim, M. Chang, and H. Hwang, *Appl. Phys. Lett.* **88**, 082904 (2006).

⁷S. C. Chen, T. C. Chang, S. Y. Chen, C. W. Chen, S. C. Chen, S. M. Sze, M. J. Tsai, M. J. Kao, and F. S. Yeh Huang, *Solid-State Electron.* **62**, 40 (2011).

⁸Y. T. Tsai, T. C. Chang, C. C. Lin, S. C. Chen, C. W. Chen, S. M. Sze, F. S. Yeh(Huang), and T. Y. Tseng, *Electrochem. Solid-State Lett.* **14**, H135 (2011).

⁹M. C. Chen, T. C. Chang, S. Y. Huang, S. C. Chen, C. W. Hu, C. T. Tsai, and S. M. Sze, *Electrochem. Solid-State Lett.* **13**, H191 (2010).

¹⁰J. J. Huang, T. C. Chang, J. B. Yang, S. C. Chen, P. C. Yang, Y. T. Chen, H. C. Tseng, S. M. Sze, A. K. Chu, and M. J. Tsai, *IEEE Electron Device Lett.* **33**, 1387 (2012).

¹¹K. C. Chang, T. M. Tsai, T. C. Chang, Y. E. Syu, C. C. Wang, S. L. Chuang, C. H. Li, D. S. Gan, and S. M. Sze, *Appl. Phys. Lett.* **99**, 263501 (2011).

¹²P. C. Yang, T. C. Chang, S. C. Chen, Y. S. Lin, H. C. Huang, and D. S. Gan, *Electrochem. Solid-State Lett.* **14**, H93 (2011).

¹³C. C. Lin, T. C. Chang, C. H. Tu, W. R. Chen, C. W. Hu, S. M. Sze, T. Y. Tseng, S. C. Chen, and J. Y. Lin, *Appl. Phys. Lett.* **93**, 222101 (2008).

¹⁴C. H. Tung, K. L. Pey, L. J. Tang, M. K. Radhakrishnan, W. H. Lin, F. Palumbo, and S. Lombardo, *Appl. Phys. Lett.* **83**, 2223 (2003).

¹⁵M. Liu, Z. Abid, W. Wang, X. He, Q. Liu, and W. Guan, *Appl. Phys. Lett.* **94**, 233106 (2009).

¹⁶H. C. Tseng, T. C. Chang, J. J. Huang, P. C. Yang, Y. T. Chen, F. Y. Jian, S. M. Sze, and M. J. Tsai, *Appl. Phys. Lett.* **99**, 132104 (2011).

¹⁷J. Yi, X. D. He, Y. Sun, and Y. Li, *Appl. Surf. Sci.* **253**, 4361 (2007).

¹⁸J. G. Choi, D. Choi, and L. T. Thompson, *Appl. Surf. Sci.* **108**, 103 (1997).

¹⁹K. Jung, H. Seo, Y. Kim, H. Im, J. P. Hong, J. W. Park, and J. K. Lee, *Appl. Phys. Lett.* **90**, 052104 (2007).

²⁰L. Goux, J. G. Lisoni, X. P. Wang, M. Jurczak, and D. J. Wouters, *IEEE Trans. Electron Devices* **56**, 2363 (2009).

²¹U. Russo, D. Ielmini, C. Cagli, and A. L. Lacaita, *IEEE Trans. Electron Devices* **56**, 193 (2009).

²²K. M. Kim, G. H. Kim, S. J. Song, J. Y. Seok, M. H. Lee, J. H. Yoon, and C. S. Hwang, *Nanotechnology* **21**, 305203 (2010).

²³S. Yu, Y. Wu, and H.-S. P. Wong, *Appl. Phys. Lett.* **98**, 103514 (2011).

²⁴S. Yu, X. Guan, and H.-S. P. Wong, *IEEE Trans. Electron Devices* **59**, 1183 (2012).